Testing resonating vector strength: Auditory system, electric fish, and noise

J. Leo van Hemmen, André Longtin, and Andreas N. Vollmayr

Citation: Chaos **21**, 047508 (2011); doi: 10.1063/1.3670512
View online: http://dx.doi.org/10.1063/1.3670512
View Table of Contents: http://chaos.aip.org/resource/1/CHAOEH/v21/i4
Published by the American Institute of Physics.

Testing resonating vector strength: Auditory system, electric fish, and noise

J. Leo van Hemmen,[1] André Longtin,[2] and Andreas N. Vollmayr[1]
[1]*Physik Department T35 & BCCN – Munich, Technische Universität München, 85747 Garching bei München, Germany*
[2]*Department of Physics, University of Ottawa, Ottawa, Ontario K1N 6N5, Canada*

(Received 21 September 2011; accepted 29 November 2011; published online 29 December 2011)

Quite often a response to some input with a specific frequency $\nu_\circ$ can be described through a sequence of discrete events. Here, we study the synchrony vector, whose length stands for the vector strength, and in doing so focus on neuronal response in terms of spike times. The latter are supposed to be given by experiment. Instead of singling out the stimulus frequency $\nu_\circ$ we study the synchrony vector as a function of the real frequency variable ν. Its length turns out to be a resonating vector strength in that it shows clear maxima in the neighborhood of $\nu_\circ$ and multiples thereof, hence, allowing an easy way of determining response frequencies. We study this "resonating" vector strength for two concrete but rather different cases, viz., a specific midbrain neuron in the auditory system of cat and a primary detector neuron belonging to the electric sense of the wave-type electric fish *Apteronotus leptorhynchus*. We show that the resonating vector strength always performs a clear resonance correlated with the phase locking that it quantifies. We analyze the influence of noise and demonstrate how well the resonance associated with maximal vector strength indicates the dominant stimulus frequency. Furthermore, we exhibit how one can obtain a specific phase associated with, for instance, a delay in auditory analysis. © *2011 American Institute of Physics*. [doi:10.1063/1.3670512]

Neurons that are driven by a periodic stimulus typically respond with a certain preference to the phase of that stimulus. It is of interest to understand the processes that govern this phase locking, and particularly the effect of noise, so as to deepen our comprehension of neuronal coding in sensory systems. A commonly used measure for the degree of phase locking is the vector strength (VS). It takes on a value near its maximum of 1 when the neuronal spike events always occur near the very same phase of the stimulus and vanishes for e.g., equidistributed spike times. The vector strength is computed by evaluating a formula[1,2] at the driving frequency. Here, we test a computational extension of the vector-strength concept[3,4] to the case that considers VS as a function of frequency, including the known driving frequency. By varying the frequency for a given and fixed set of spike times or, more generally, events stemming from experiment, here from the cochlear nucleus of cats and electroreceptors of brown ghost electric fish, we see a resonance behavior as the frequency variable moves through the input frequency. Hence, we need not even know the latter and call the notion we focus on "resonating vector strength" (RVS). We show explicitly that RVS reveals a resonating structure, dominated by a main peak with multiple side peaks. The shape of the resonating vector strength agrees with a theoretical description. In particular, supporting theory makes RVS useful for assessing the statistics of the noise process that can jitter the firing phases, and even randomly remove spikes from certain driving cycles when the period of the drive is short enough to interfere with the recovery of the neuron following a spike. Our analysis also shows that both types of data exhibit a maximal VS at a frequency that can differ from that at which the cell is stimulated. It highlights the importance of looking at the RVS from individual runs, where the assumption of independence of the noise perturbations at different spike times appears to break down.

I. INTRODUCTION

The vector strength[1–3] quantifies the amount of periodicity in a neuronal, or any other, response to a given periodic signal. We denote a neuronal response by a sequence of spike times, in a more general context also called events, $\{t_1,t_2,\ldots,t_n\}$ where in what follows $1 \le j \le n$ labels the spikes and in general $n \gg 1$. Actually, the vector strength is the length of the synchrony vector[3] or the absolute value of the complex number $(i = \sqrt{-1})$

$$\rho(\omega) = \frac{1}{n}\sum_{j=1}^{n} e^{i\omega t_j}. \tag{1}$$

Here, $\omega = 2\pi/T$ denotes an angular frequency for some period T. What (1) does is to put the spike times t_j or more precisely the dimensionless times t_j/T onto a circle with radius 1, the appropriate temporal domain for phenomena of period T. Since after 2π we are back at where we started on the unit circle, we multiply t_j/T by 2π so as to get $2\pi t_j/T = \omega t_j$, put ωt_j onto a unit circle by means of $\exp(i\omega t_j)$, and arrive at Eq. (1).

Let us take all times t_j to be integer multiples of some period $T_\circ$; say, $t_j = jT_\circ + \delta$ where we have also added some common constant δ, which may, for example, stand for a delay. Then $\omega_\circ T_\circ = 2\pi$ and we see that whatever j we get for all

times t_j, which we henceforth call "spike times" or "spike events," $\exp(i\omega t_j) = \exp(i\omega\delta)$ and thus $\rho(\omega_\circ) = \exp(i\omega_\circ\delta)$, which has absolute value 1. The quantity $r = |\rho(\omega_\circ)|$ is the traditional vector strength,[1,2] which only considers $\omega = \omega_\circ$ in Eq. (1).

Conversely, one can show that for $r = |\rho(\omega)| = 1$ we are bound to find $t_j = jT + \delta$ for the period T corresponding to ω. To see why, we note that the fundamental vector-strength lemma [Ref. 3, Lemma] says that for $r(\omega) = |\rho(\omega)|$ we have

$$\frac{1}{n}\sum_{\ell=1}^{n} |\rho(\omega) - \exp(i\omega t_\ell)|^2 = 1 - r^2(\omega). \tag{2}$$

If for some ω we obtain $r = 1$, then all the $\exp(i\omega t_\ell)$ are bound to equal the very same $\rho(\omega)$, which is therefore on the unit circle. The δ in $t_j = jT + \delta$ corresponds to the phase indeterminacy when the absolute value $r = |\rho(\omega)| = 1$ has been fixed. Skipping a multiple of T is of course also allowed, as $|\exp[i\omega(t_j + \ell T)]| = |\exp(i\omega t_j)| = 1$ will not change if ℓ is an integer. Moreover, exploiting the afore-mentioned lemma (2) we see that for $r(\omega) = |\rho(\omega)| \to 1$ the cloud of $\exp(i\omega t_j)$ with $1 \le j \le n$ and in general $n \gg 1$ contracts in the mean to a single point on the unit circle; cf. Fig. 1(a). That is, nearly all $\exp(i\omega t_j)$ must do so.

A neat aspect of the unit circle is its simple, toroidal geometry: After one walk around we are automatically back at where we started, just like after one oscillation period. It was von Mises[1] who realized as early as 1918 that an appealing way of looking at the problem of measuring periodicity of points t_j on the real axis is putting them on the unit circle through $t_j \mapsto \exp(i\omega_\circ t_j)$ and taking the position of their center of mass or barycenter $\rho(\omega_\circ) = \left[\sum_{j=1}^{n} \exp(i\omega_\circ t_j)\right]/n$ as a criterion for the goodness of fit. As we see in Eq. (2), the nearer $r(\omega_\circ) = |\rho(\omega_\circ)|$ is to 1, the better the periodicity of the response $\{t_1, t_2, \ldots, t_n\}$. The rest is convex geometry.[3]

The procedure we follow is straightforward in that for *given* spike events t_j belonging to a run $1 \le j \le n$ we vary the frequency ω in Eq. (1) and study $\rho(\omega)$'s response (on the computer). This we call the *resonating* vector strength. We will soon see that "resonating" is not an epithet and also understand why; see Fig. 1(b) for an illustration.

The number n of spikes involved in a run is nearly always large, corresponding to experimental times $T_{\rm ex}$ much longer than the neuronal ones, which in practically all neuronal systems are of the order of a millisecond or shorter. So $T_{\rm ex} \gg 1$ ms and accordingly $n \gg 1$. When applying an "external" angular frequency $\omega_\circ$ one usually[1,2] substitutes $\omega = \omega_\circ$ into Eq. (1) and evaluates this expression for several runs, each giving a resulting position, a complex number or 2-dimensional vector in a vector-strength plot like Fig. 1(a). Taking the arithmetic mean of all positions we obtain an average, the *synchrony vector*,[3] whose absolute value is traditionally called the *vector strength*. It results from the total, composite, experiment consisting of all runs or, in other words, of all the repetitions of the very same experiment.

The present work consists of three parts. First, we evaluate the resonating vector strength (1) as a function of ω or $\nu = \omega/(2\pi)$ for a periodically responding neuron with $t_j = jT_\circ + \delta$ and then test its behavior by comparing it with a full set of data due to Joris *et al.*,[6] for a *given* set of spike events stemming from an auditory neuron in the cat's anterior ventral cochlear nucleus (AVCN) in response to input frequencies $\nu_\circ = m \times 100$ Hz with $1 \le m \le 24$. The AVCN is one of the cochlear nuclei situated directly after the cochlea, while the trapezoid body (TB) is the next station after the cochlear nuclei. By taking advantage of the resonating vector strength (RVS) we can see at a glance (Figs. 2 and 3) that this AVCN neuron, presumably—the authors[6] do not know this for sure but we will stick to it without any further

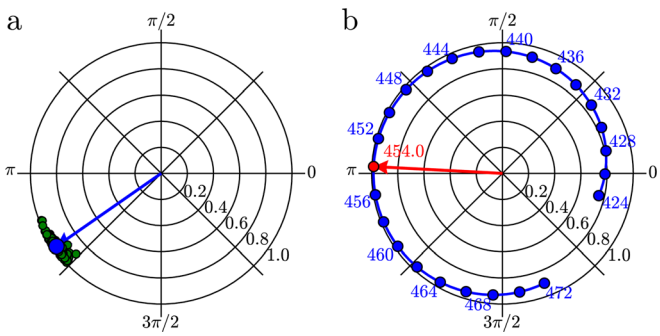

FIG. 1. (Color online) (a) Synchrony vector resulting from several runs recorded in the trapezoid body (TB), the station following the ventral cochlear nucleus, here in cat. The frequency of the auditory stimulus in the experiment as described by Joris *et al.*[6] was $\nu_\circ = 460$ Hz, which has been substituted into Eq. (1). On the left in (a) we see both the separate synchrony vectors (indicated by dots in the complex plane so that the phase comes for free) and the resulting vector strength (for short VS for the length of the vector) as the arithmetic mean of 50 TB responses giving VS = 0.98. As is evident from the plot, the scatter of the different dots is indeed low but its origin is not really known. The duration $T_{\rm ex}$ of each run [Ref. 6, Fig. 1] was about 25 ms so that $n = 12$ in Eq. (1). (b) By varying ω or equivalently ν in Eq. (1) we see on the right how $r = |\rho(\nu)|$ becomes maximal or "resonant" for a specific frequency $\tilde{\nu} = 454.0$ Hz with $r = |\rho| = 0.98$ but with $\tilde{\nu}$ near to but yet different from the input frequency $\nu_\circ = 460$ Hz. For $\nu = 460$ Hz the argument or phase δ of $\rho(\nu)$ is the same in both plots. Both in (a) and in (b) the spike data are due to Joris *et al.*[6] and the plots stem from Ref. 4.

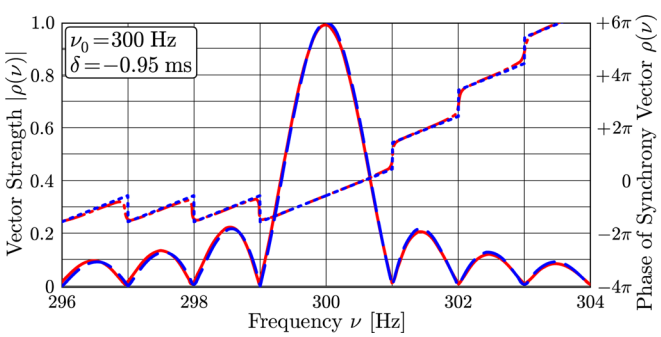

FIG. 2. (Color online) Resonating vector strength (RVS, solid line) $|\rho(\nu)|$ as a function of the frequency ν for spike data obtained from a globular bushy cell in the cochlear nucleus for auditory-nerve input frequency $\nu_\circ = 300$ Hz. The long-dash line coincident with the solid curve is the theoretical prediction (4). RVS scale on the left and phase scale on the right, with dotted lines for the theoretical prediction of the phase also due to Eq. (4) and dot-dashed line for experiment; the jumps $\pm\pi$ are due to sign changes of $\mathcal{S}$]; RVS($\nu_\circ$) = 0.99. The long-dash line is the ideal response (4) with $|\mathcal{S}|$ for perfect locking with a periodic stimulus of frequency $\nu_\circ$. As compared with Fig. 1, the resonance as a function of ν is quite sharp while the underlying $\nu_\circ$ is again exactly at the (absolute) maximum of the center peak. Hence, it is fair to say that $|\rho(\nu)|$ is truly resonating at $\nu_\circ = 300$ Hz. The spike data is due to Joris and Smith[7] and the plot to Ref. 4.

comment—a globular bushy cell (GBC), phase-locks perfectly to any input frequency as long as it can lock, so to speak. If the input frequency $\nu_\circ$ becomes too high, then phase locking stops in the auditory system of mammals.

Second, noise is omnipresent in neuronal systems. Here "noise" stems from sources we mostly do not know or cannot characterize precisely and therefore model through noise. One can implement noise straightforwardly by adding a random time δ_j' to the event times t_j; say, the δ_j' are independent, identically distributed random variables with mean $=0$, standard deviation σ, and some distribution that we need not specify yet. Noise deteriorates neuronal response but how does it modify the RVS behavior? This is a question we will try to analyze and answer through a comparison with full data sets of Joris *et al.*,[6] and Joris and Smith.[7]

Third, we turn to the weakly electric fish *Apteronotus leptorhynchus*, also known as the brown ghost knife fish. This wave-type electric fish generates a quasi-sinusoidal electric field oscillation with a fixed and highly periodic frequency in the range 600–1000 Hz using the electric organ in its tail; see Chacron *et al.*,[8] for background information. Wave-type weakly electric fish, in which the active sensing uses a quasi-sinusoidal waveform, is distinguished from pulse-type fish, which emit pulses of electric current in an almost periodic manner to actively sense their environment. The wave-type fish behaves essentially as an oscillating electric dipole. The electric sense of the brown ghost induces dipolar oscillations in the environment. These "object" oscillations then alter the local electric organ discharge (EOD) amplitude at the skin. Thus, the objects produce an electric image, which is perceived by electroreceptors dispersed over the skin, and especially in the head region. These electroreceptors are continually driven by the EOD, whose amplitude is modulated by the field it induces in objects.

When an object has a conductivity that differs from that of the surrounding water, the electric field lines are distorted, and the amplitude of the EOD carrier wave is decreased or increased depending on whether the conductivity has gone down or up. We focus below on the tuberous p-unit type of electroreceptor associated with this EOD-generated *active* electric sensing, in contrast to ampullary electroreceptors that are associated with passive electrosensation and exhibit noisy phase-locked behavior to internally generated receptor oscillations.[11] These p-units—or "probability coders" since their firing probability increases with local carrier-amplitude modulations—signal the deviation of the electric field from its baseline pattern on the skin. The electric organ discharge (EOD)-induced image as observed by the fish's electroreceptors dispersed over the body surface is comparable with that perceived by the lateral line observing[12] a hydrodynamic image generated by objects, e.g., predator or prey, in its direct surroundings in that it is diffuse, distributed all over the body.

Each electroreceptor increases its firing rate in proportion to the instantaneous local EOD amplitude. On a finer time scale, firings actually show a phase locking to the EOD. More precisely, the EOD induces a stochastic phase-locked firing pattern with randomly skipped cycles[9] that is very similar to the one seen in auditory afferents of cat.[10] Increases in EOD produce a higher rate of these noisily phase-locked spikes. Plots of vector strength (VS) as a function of frequency have been used occasionally in the neurophysiology literature, in particular, in the context of electroreception.

What we are doing here is different: We assume the cell is stimulated by the EOD at a frequency $\nu_\circ$ without amplitude modulation. The RVS (1), however, is evaluated at the frequency $\nu_\circ$ *plus* neighboring "test" frequencies ν but without changing the driving frequency (which is under the fish's control, as opposed to the auditory experiments where it is under the experimenter's control) nor the spike times t_j responding to $\nu_\circ$. One can then produce a polar plot of $\rho(\omega)$ as given by Eq. (1) or equivalently $\rho(\nu)$, parameterized by the test frequency or simply the real variable $\nu_\circ$, or plot the magnitude or phase of $\rho(\nu)$ as a function of the test frequency over a whole range of ν; cf. Figs. 2, 3, 5, and 6. As we will see in Sec. IV, this produces a finer probing of the phase locking properties at each frequency.

II. VECTOR STRENGTH RESONATING IN A PERFECTLY PERIODIC RESPONSE

Using Eq. (1), we now evaluate $\rho(\omega)$ as a function of the real variable ω in the case where the spikes respond *perfectly* to an input of angular frequency $\omega_\circ = 2\pi\nu_\circ = 2\pi/T_\circ$ so that $t_j = jT_\circ + \delta$ with some fixed phase δ. Then $\omega_\circ t_j = \omega_\circ(jT_\circ + \delta)$ and thus $\rho(\omega_\circ) = \exp(i\delta\omega_\circ)$ as we are on the unit circle. Realizing ρ's dependence upon the variable ω and writing $\omega = (\omega_\circ + x)$ we obtain[4] after some straightforward algebra associated with handling geometric series,

$$\rho(x) = \frac{e^{i\omega\delta}}{n}\left[\sum_{j=1}^{n} e^{ijxT_\circ} = e^{i(n+1)xT_\circ/2}\frac{\sin(xnT_\circ/2)}{\sin(xT_\circ/2)}\right]. \quad (3)$$

In the case of perfect resonance producing n spikes with a period $T_\circ$, the experiment lasts $T_{\rm ex} = nT_\circ$. Later on we will analyze the situation where $T_{\rm ex} = NT_\circ$ but $n < N$. Without loss of generality we can, and will, put $\delta = 0$ most of the time.

Because in Eq. (3) there is a $1/n$ waiting for what follows on the right of it we rewrite the perfectly locking (3) in the form

$$\rho(x) = e^{i[\omega\delta + x(T_{\rm ex}+T_\circ)/2)]}\left[\frac{\sin(xT_{\rm ex}/2)}{n\sin(xT_{\rm ex}/2n)} = \mathscr{S}(x)\right]. \quad (4)$$

As for zeros and decrease in absolute value of $\rho(x)$ as we move away from $\nu_\circ$ or $x = 0$ in Eq. (4), it suffices to focus on $\mathscr{S}(x)$. We see a fast decrease of $\rho(x)$'s absolute value. As a prelude to what follows we show in Fig. 2 a plot of the vector strength $r = |\rho|$ as a function of x or effectively $(\nu - \nu_\circ)$ for an input frequency of $\nu_\circ = 300$ Hz. We cannot even discern the solid from the long-dash line, i.e., the resonating VS based on given spike events t_j or events and averaged over 50 runs of 1 s each, from the ideal response $|\mathscr{S}|$ for perfectly periodic events. That is, the resonating vector strength does what its name says: It neatly resonates, so to speak, at $\nu_\circ$ or $x = 0$.

As is evident from Eq. (3), $|\rho(0)| = 1$ and $|\rho(x)|$ decreases fast as a function of x. To see why, we note that the first zeros of $\mathscr{S}(x)$ already appear when $xnT_\circ/2 = \pm\pi$ or equivalently $xT_\circ/2 = \pm\pi/n$. Accordingly, due to the

definition $x = 2\pi(\nu - \nu_\circ)$ and the fact that $T_{\rm ex} = 1$ s for the experimental situation of Fig. 2, we find $(\nu - \nu_\circ)T_{\rm ex} = \pm 1$ and hence $\nu - \nu_\circ = \pm 1$ Hz for reaching the first zeros surrounding $x = 0$, where $|\rho(0)| = 1$ is the absolute maximum.

For perfect locking with a periodic signal, the relative maxima of $|\mathscr{S}(x)|$ and hence $|\rho(x)|$ occur at $xT_{\rm ex}/2 = \pm k\pi/2$ with $k \geq 3$ odd. Since n is large we obtain to decent precision (or better) $n \sin(xT_{\rm ex}/2n) = xT_{\rm ex}/2$ in the neighborhood of $x = 0$ and with $xT_{\rm ex}/2 = \pm k\pi/2$ the relative maxima of $|\rho(x)|$ turn out to be $2/(k\pi)$, in exact agreement with Fig. 2.

Equation (4) also allows us to determine $\delta \neq 0$ quite straightforwardly since the phase factor in front of $\mathscr{S}(x)$ reads $\exp\{i[\omega\delta + x(T_{\rm ex} + T_\circ)/2)]\}$ with $x = \omega - \omega_\circ = 2\pi(\nu - \nu_\circ)$. Since $\mathscr{S}$ is smooth, $|\mathscr{S}|$ has a jump in the derivative when $\mathscr{S}(x)$ becomes negative as $xT_{\rm ex}/2$ passes $\pm k\pi$ for $k \geq 1$, the phase shows a discontinuity of π at the zeros of $\mathscr{S}$, and thus we see π jumps occurring in the phase plot of Fig. 2.

If we have a decent phase locking we expect[3] a relatively small cloud of $\exp(i\omega_\circ t_j)$ around some $\exp(i\omega_\circ\delta)$, and this is what Fig. 1(a) shows. When ω moves away from $\omega_\circ$ the vectors $\exp(i\omega t_j)$ start diffusing on the unit circle and, depending on $n \gg 1$, their arithmetic average quickly becomes quite small, as Eq. (4) and Fig. 2 indicate explicitly. As soon as the phase locking stops functioning with increasing input frequency $\nu_\circ$ and as soon as the time shift δ_j in $t_j = (jT_\circ + \delta_j)$ depends on j with the δ_j being practically independent random variables, we expect a decrease of $|\rho(x)|$ both at $x = 0$ for increasing $\nu_\circ$ and as x moves away from 0 for fixed $\nu_\circ$. Equation (5) below presents an illustration of what then happens. We are going to analyze whether and how noise can describe the change in neuronal behavior, here of the auditory system, when the input frequency increases even beyond the boundary where phase locking makes sense physically.

III. RESONATING VECTOR STRENGTH IN THE PRESENCE OF "NOISE"

Life is not perfect and we imagine "noise" to characterize what we cannot specify precisely but can model mathematically. For the moment, we assume the events t_j are generated by some deterministic process, such as $t_j = jT_\circ$, but note the t_j need not be periodic at all. The events themselves are related to the previously discussed auditory process. We will focus on the brown ghost electric fish in Sec. IV. On top of these deterministic events there is additive noise δ'_j modifying each t_j so as to give as outcome $t_j + \delta + \delta'_j$ that is to be substituted into Eq. (1). For the time being we put $\delta = 0$. As for the δ'_j, we assume they are identically distributed random variables with zero mean, either independent[13–15] or practically independent in the sense that they have short-range correlations as j varies. The latter assumption is quite natural to phenomena in biological physics and means that we can still apply both the strong law of large numbers and the central limit theorem or, for short, the laws of large numbers; for fairly optimal conditions we refer to elsewhere (Ref. 5, Appendix A).

Let μ be the probability distribution of the δ'_j so that its characteristic function is given by $F(\omega) = \int {\rm d}\mu(\delta') \exp(i\omega\delta')$; by its very definition $|F(\omega)| \leq 1$. Upon substituting $t_j + \delta'_j$ into Eq. (1) we find, up to a Gaussian error of order $1/\sqrt{n}$ due to the central limit theorem[15] and indicated below by $\doteq$,

$$\rho(\omega) \doteq \left(\frac{1}{n}\sum_{j=1}^{n} e^{i\omega t_j}\right) F(\omega) =: \rho_{\rm w/o\ n}(\omega) F(\omega). \qquad (5)$$

Here, $\rho_{\rm w/o\ n}$ is the synchrony vector $\rho(\omega)$ *without* noise as we see it in Eq. (3). The above multiplicative expression (5) is a consequence of the identical distribution of the δ'_j and the self-averaging of Eq. (1) is due to their short-range correlations. In passing we note that the neuron still is to respond to each period of the oscillating stimulus.

We now turn to Fig. 3. It is a 3-dimensional plot of analogs of Fig. 2 one behind the other starting with stimulus frequency $\nu_\circ = 100$ Hz and $\nu_\circ$ increasing in steps of 100 up to 1500 Hz. Experimentally, this corresponds to choosing a stimulus frequency $\nu_\circ$, and obtaining a spike train. For this spike train, which is now given and fixed, one calculates the RVS in which the driving frequency $\nu_\circ$ is set at that value, and the probing frequency ω (under the control of the person analyzing the data) is swept over a smaller or larger range around $\nu_\circ$. Then, the whole procedure is repeated choosing a different value of the driving frequency $\nu_\circ$. This purely computational procedure is readily done in, e.g., auditory

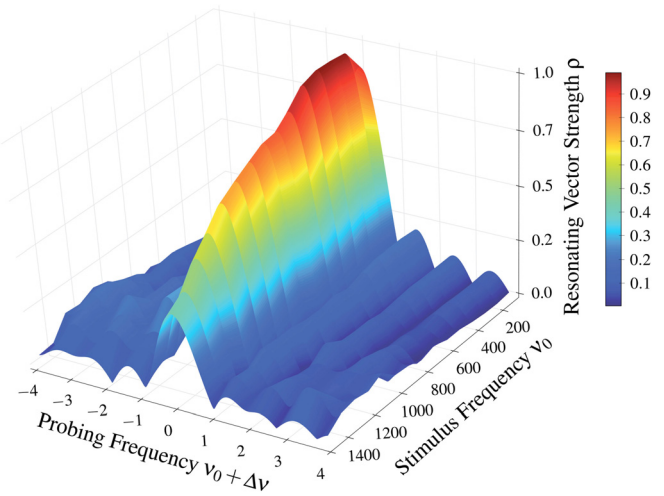

FIG. 3. (Color online) 3-Dimensional plot of the resonating vector strength (RVS, vertical axis) as a function of the "probing" frequency $\Delta\nu$ around the stimulus frequency $\nu_\circ$ for spike data obtained from a globular bushy cell in the cochlear nucleus for auditory-nerve stimulus frequencies $\nu_\circ = 100, \ldots, 1500$ Hz, from back to front; of course $\nu = \nu_\circ + \Delta\nu$ with $\omega = 2\pi\nu$ as it occurs in Eq. (1). The experimental sound level was 80 dB SPL. The spike events t_j are the response to the (varying) stimulus frequency $\nu_\circ$, hence given by experiment and fixed for all the runs. For each $\nu_\circ$ there are 15 runs and the plotted RVS is their arithmetic mean; see Fig. 5 for how the RVS of the individual runs may look. Focusing on the vertical plane through $\Delta\nu = 0$ and parallel to the stimulus frequency $\nu_\circ$ axis, we see that $r = |\rho(\nu_\circ)|$ increases rather steeply from 0.88 at $\nu_\circ = 100$ Hz to 0.98 at $\nu_\circ = 200$ Hz and stays at its maximum (practically) 1 between 300 and 500 Hz. The RVS as evaluated at $\nu_\circ$, where it always assumes its absolute maximum, then decreases from 1 via 0.40 at $\nu_\circ = 1500$ Hz and shown in Fig. 5(d) to effectively 0 at 2400 Hz (not shown here but appearing as Fig. 3(b) in Joris *et al.*[7]); the present figure stops at the front with $\nu_\circ = 1500$ Hz as border line. The line coincident with the factual response at $\nu_\circ = 300$ Hz, which is the plot of Fig. 2, is the expression $|\mathscr{S}|$ in Eq. (4) for perfect locking. The spike data are due to Joris and Smith.[7]

experiments, where the driving or "carrier" frequency is under the experimental control and varies in a natural setting.

In the case of the electric fish studied here, the driving frequency $\nu_\circ$ is under the fish's control, i.e., it is set by its internal pacemaker producing the EOD at frequency $\nu_\circ$. For a given time interval, say, the duration of the experiment $[0, T_{ex})$, one can do only a single computation of RVS as a function of the probing frequency ω. Alternatively, as we will see in Fig. 6, we can always split up $[0, T_{ex})$ into finitely many subsequent subintervals and compute the RVS for each subinterval in addition to the total one for the whole interval. In other wave-type species (such as *Eigenmannia*), the EOD is disabled by the anesthetic and has to be synthesized using mouth and tail electrodes—in this case $\nu_\circ$ would also be under the experimenter's control and a full plot like in Fig. 3 could be produced.

Three aspects of Fig. 3 deserve our attention. First, $r = |\rho(\nu_\circ)|$ increases rather steeply from 0.88 at $\nu_\circ = 100$ Hz to 0.98 at $\nu_\circ = 200$ Hz, stays at its maximum (practically) 1 between 300 and 500 Hz, and then slowly decreases to 0.4 at 1500 Hz (see also Fig. 6(d)); though not shown, it continues decreasing until it vanishes beyond $\nu_\circ = 2400$ Hz. In fact, the line of maxima for $100 \le \nu_\circ \le 1500$ Hz is identical with Fig. 3(b) of Joris and Smith,[7] who show the whole range, up to and even beyond $\nu_\circ = 2400$ Hz. In passing we note that Fig. 3(a) of Joris and Smith[7] presents a color code of loudness (SPL) for the different stimuli.

Second, the increase of $r = |\rho(\nu_\circ)| = 0.88$ at $\nu_\circ = 100$ Hz to 0.98 at $\nu_\circ = 200$ Hz looks and in fact is a bit surprising. The neurobiological explanation is a kind of "spike doubling" in that for 100 Hz we see every now and then two spikes per period, a second one on the average 1.8 ms after the first, instead of a single one every 10 ms, whereas for $200 \le \nu_\circ \le 500$ Hz we find one and only one perfectly locked spike per period, as Fig. 2 and the single runs of, e.g., Fig. 5(a) show. Not only do the high values (≥ 0.4) of $r = |\rho(\nu_\circ)|$ for $100 \le \nu_\circ \le 1500$ Hz indicate that globular bushy cells are very broadly tuned. With respect to the auditory nerve they in fact strongly increase the coherence with the external stimulus, here a pure tone of frequency $\nu_\circ$, and in so doing greatly improve the "quality" of entrainment [Ref. 7, Fig. 1] in the whole low-frequency range where cochlear neurons (of mammals such as cat) can perform phase locking.

Third, whereas in Fig. 2, the agreement between the theoretical (long-dash) curve and the experimental (solid) line is perfect for $\nu_\circ = 300$ Hz, there are already clear deviations from Eq. (5) for, say, $\nu_\circ = 1000$ Hz. Here, the relative maxima of $|\rho(\omega)|$ are to be located at $xT_{ex}/2 = \pm k\pi/2$ with $k \ge 3$ odd. Since by definition $x = 2\pi(\nu - \nu_\circ)$ we expect the relative maxima at $(\nu - \nu_\circ) = \pm k/(2T_{ex})$, which is about right. The minima, however, ought to be zero $(=0)$ at $xT_{ex}/2 = \pm \ell\pi$ with $\ell \ge 1$ a natural number (like k) since ρ in Eq. (5) is the *product* of $\rho_{w/on}$ and F. Quite often reality is different in that the minima of $|\rho(\nu)|$ are located at $(\nu - \nu_\circ) = \pm \ell/T_{ex}$ to decent approximation but > 0. Why is that?

A. Skipping: When phase locking drops out

After having produced an action potential, a neuron experiences a refractory period (Ref. 17, Sec. 6.3.2] during which it cannot fire; this is known as the absolute refractory period. Following this period, the strength of the stimulus that can induce an action potential decreases monotonically to some asymptotic level. This is the relative refractory period. In the neurons of interest here, the sum of these two periods, i.e., the total refractory period, lasts typically 0.5–2 ms. So an auditory neuron cannot phase lock perfectly in the sense that it cannot fire after each period once the input frequency $\nu_\circ$ gets too high. Then it has to leave, so to speak, a "hole" in the sequence $jT_\circ$ and skip one or more periods. That is why we call this phenomenon *skipping*. A famous example is the barn owl, which in this sense[18] performs phase locking up to

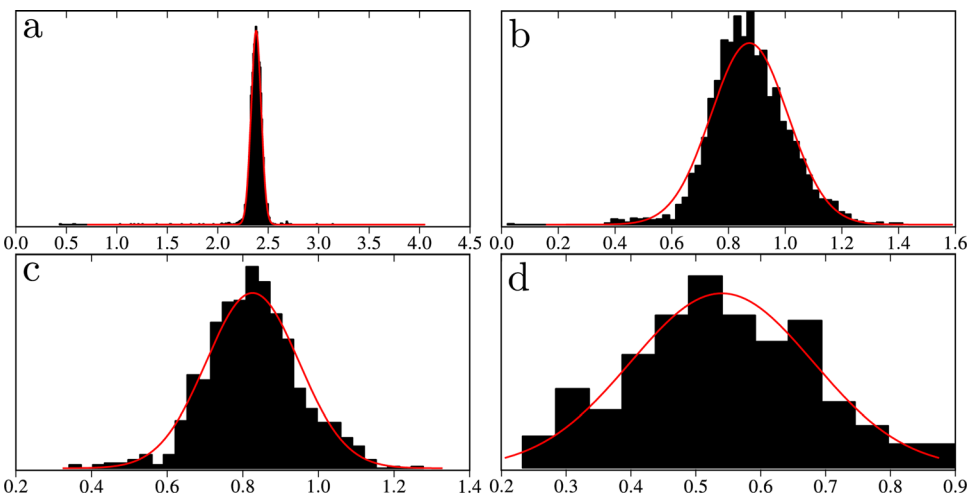

FIG. 4. (Color online) (a)–(d) Distribution of spike events t_j reduced to the interval $[-T_\circ/2, T_\circ/2)$, or a suitable part of the horizontal axis (in ms), by subtracting (or adding) as many multiples of the period $T_\circ = 1/\nu_\circ$ as are needed to land in the interval. Equivalently and far more efficiently,[1] we can consider everything on the unit circle or torus through $\exp(i\omega_\circ t_j)$ where $\omega_\circ = 2\pi/T_\circ$ as usual. For $\nu_\circ = 300$ Hz we see a narrow—in the sense that its standard deviation σ satisfies $\sigma \ll T$ – (absolutely) continuous, normal distribution but, as $\nu_\circ$ increases, the normal distribution becomes broader as we increase $\nu_\circ$ to 700, 1000, and 1500 Hz (left to right, and top to bottom), and settles on the torus. Hence, we need to take a von Mises distribution[1,22] or a wrapped Gaussian.[22] In all cases, the solid line is the Gaussian fit. The spike data underlying the above spike-time histograms are those of Figs. 2 and 3.

8–9 kHz. For mammals such as cat, the experimental animal of Figs. 1–3, the phase-locking upper bound is much lower, viz., 1.0–1.5 kHz.

Skipping phenomena have received a lot of attention in modeling studies; see e.g., Longtin and Chialvo[19] and references therein. When an oscillator is driven by an external force that is sufficiently fast, there is a competition between the time scale of the forcing and those of the internal oscillation (the latter depending on the total refractory period). There is a well-known universal organization of the n:m synchronization patterns that results, in which there are m responses (or cycles) of the oscillator to the n cycles of the input drive. When the patterns are displayed as a function of the ratio of drive to internal frequency and the drive amplitude, the familiar Arnold tongue structure appears. For example, periodic 1:1 firing is most prevalent in this parameter space, and when the forcing is too fast, every second spike response drops out, leading to a periodic 2:1 pattern.

This picture applies to a neuron that fires spontaneously as an oscillator under the influence of periodic forcing. The picture also applies, but with some minor qualitative differences, when the neuron is excitable, i.e., when it is spontaneously at rest. But noise will blur the boundaries of the region corresponding to a given n:m pattern. In fact, because an excitable neuron becomes a stochastic oscillator in the presence of noise, this noise is also extends the deterministic Arnold tongues into the subthreshold regime. When the noise is significant, as it appears to be in the systems studied in this paper, there is no clear signature of one mode locked pattern, but rather a random mix of such patterns that produce, e.g., multi-peaked interspike interval histograms with a smooth unimodal envelope.[19] A further investigation of the predominance of certain mode locked patterns would likely benefit from the measure of stochastic phase synchronization indices as in Bahar *et al.*[20]; see also Eqs. (8) and (9) below. Here, we focus on understanding our RVS results in terms of simple stochastic descriptions of the firing behaviour. As we will see, interestingly some assumptions break down at higher frequencies.

Stochastic modeling—How do we model the skipping of events in a regular series $t_j = jT_\circ$, $j \geq 1$? It is plain that this skipping has its influence on the outcome of the sum $\rho(\omega) = \left[\sum_{j=1}^{n} \exp(i\omega t_j)\right]/n$. To quantify this influence analytically we make the simplest possible assumption and assume that each spike occurs with probability p and does not occur with probability $1-p$. Surprisingly, it works smoothly. A similar argument was made to explain the asymptotic exponential decay of the peaks of the interspike interval histogram (ISIH) for certain kinds of skipping data.[10] We then multiply $\exp(i\omega t_j)$ by an independent random variable ζ_j that is 1 or 0 with probability p or $(1-p)$. In this way, we get a sequence of independent, identically distributed (iid) random variables ζ_j and simply find, as n becomes large, the product $p\rho_{\text{w/o n}}$ by the strong law of large numbers;[15] cf. Eq. (6) below. We now spell out how and why.

Before proceeding we note that it may be more realistic to describe skipping not by a simple uniform probability p but instead by conditioning with respect to the event that we just had a spike. If so, a Markov *Ansatz* would be quite natural. Be that as it may, a simpler, self-consistent, and surprisingly well functioning argument à la Occam's razor is assuming independence or short-range correlations of the spiking events. In so doing we will see that skipping is far more pronounced than we might naively expect but that we nevertheless end up with Eq. (5).

We first bring in the total time $T_{\text{ex}} = NT_\circ$ of the experiment. Since the neuron skips certain firing times, the resulting number of spikes is not N but by its very definition $n < N$ as the probability $p < 1$ of getting a spike is less than 1 and $N \gg 1$. We start by evaluating

$$\rho(\omega) = \frac{1}{n}\sum_{j=1}^{N} \zeta_j \exp[i\omega(jT_\circ + \delta_j')]. \tag{6}$$

Here n is, as always, the actual number of spike events, which are counted by the 0-1 random variable ζ_j. So n is a random variable itself. In Eq. (6) we have at least two

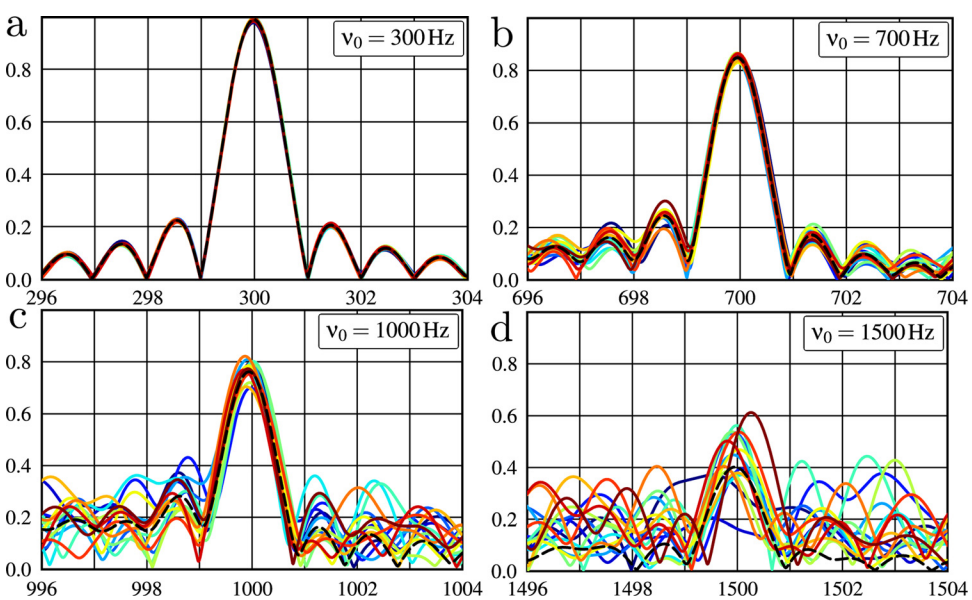

FIG. 5. (Color online) Plots of $\rho(\nu)$ as a function of the frequency ν in the neighborhood of the auditory stimulus frequency $\nu_\circ = 300$, 700, 1000, 1500 Hz for 15 *separate* runs, left to right and top to bottom. In contrast to Figs. 1–3, where in 2 and 3 we have used data from the same neuron and in all taken an arithmetic mean of the different runs, we now see each of them separately. Whereas there is perfect locking and a practical coincidence of the separate runs for $\nu_\circ = 300$, we note a gradually augmenting discrepancy between the different runs as $\nu_\circ$ increases, indicating the irregular ("stochastic") skipping of spikes. The mean number $\langle n \rangle$ of spikes has been obtained from the same spike data as those of Figs. 2 and 3, which are due to Joris and Smith,[7] who have also plotted $\langle n \rangle$ as a firing rate (for 1 s) against the stimulus frequency $\nu_\circ$ in their Fig. 3(c).

processes, which to a large extent are independent. First, neuronal skipping, which we model by the 0-1 variable ζ_j assuming only the two values 1 and 0 with probability p and $(1-p)$. A second process, among others that we need not model here, is the stochastic cochlear response[21] described by the random phase δ'_j, which by its very nature gives rise to an imperfect phase locking; cf. Fig. 4. As $N \to \infty$ we apply the strong law of large numbers to the ζ_j, and even though the product $\exp[i\omega(jT_\circ + \delta'_j)]\zeta_j$ is not identically distributed because of the exponential prefactor, we find [Ref. 15, Sec. 8, Theorem 3] that the above sum (6) converges to the nonrandom limit

$$\rho(\omega) = \frac{1}{n}\sum_{j=1}^{N} \exp[i\omega(jT_\circ + \delta'_j)] \doteq \rho_{\mathrm{w/o\ n}}(\omega)F(\omega). \qquad (7)$$

since $\langle\zeta_j\rangle = p$. In the transition from Eqs. (6) to (7) we have written $1/n = (N/n) \times 1/N$ and focused on $N^{-1}\left[\sum_{j=1}^{N} \ldots\right]$. By the very same strong law of large numbers the number of spikes that occur equals $n = pN$, p drops out, and we are left with the product $\rho_{\mathrm{w/o\ n}}(\omega)F(\omega)$ up to fluctuations. Since we have n terms in the remaining sum, its fluctuations are of order $1/\sqrt{n}$.

Naively, we expect that the above n in Eq. (6) is hardly less than N. In the AVCN neuron of Fig. 3 this is not always the case. We find for the 15 runs,[7] each lasting 1 s, for $\nu_\circ = 300$ Hz an arithmetic mean $\langle n\rangle$ of 300 spikes whereas for $\nu_\circ = 1000$ Hz it is just 67 and for $\nu_\circ = 1500$ Hz we are left with as little as 31; these numbers just illustrate the surprising behavior shown in Fig. 3(c) of Joris and Smith.[7] Adopting a traditional stochastic formalism we may expect a $\sqrt{n}$ fluctuation for a single run. Averaging 15 positive quantities gives a fluctuation of the same magnitude since the location of the minima is fixed. And that is what we observe in Fig. 3.

If for a given stimulus frequency $\nu_\circ = 1500$ Hz the arithmetic mean $\langle n\rangle = 31$ of the spike events occurring during $T_{\mathrm{ex}} = 1$ s is that low, a neuron must "skip" quite a few of the 1500 periods that occur. How, then, can we understand this skipping? That is, how to interpret the above formalism? An even more urgent question is how to understand a neuron's "slippery" behavior as the stimulus frequency $\nu_\circ$ becomes large. We turn to the latter question first and then treat the former in Subsection III C.

B. Imperfect phase locking

On the mere basis of cochlear mechanics and its neuronal pickup we already expect the higher the input frequency $\nu_\circ$, the less perfect the phase locking. In principle this could be taken care of by Eq. (5) where $F(\omega) = \int \mathrm{d}\mu(\delta')\exp(i\omega\delta')$. If $\delta' = \pm\delta_0$ with probability 1/2, then $F(\omega) = \cos(\omega\delta_0)$ would never converge to 0 as ω becomes large. In the case of Figs. 1–3, however, the probability distribution of δ' is not discrete but (absolutely) continuous, even Gaussian to quite a decent extent; see Fig. 4. By the Riemann-Lebesgue lemma[16] $F(\omega)$ goes to zero as ω becomes large and accordingly $|\rho(\omega)|$ is bound to go to zero as $\omega \to \infty$.

C. Imperfect phase locking and neuronal skipping

Let us try to summarize what we have found. When a pure tone, say, one of the 24 in Fig. 3, is presented to the cochlea, the cochlear response is highly sensitive but not perfect in the sense that it does not catch the maximum of the pressure wave exactly. To fair approximation a decently locked neuronal response can be described by a Gaussian with small standard deviation with respect to the period but, since a pure tone is "purely" periodic, we need to put the probability distribution on a torus. We then get a wrapped Gaussian[22] or, analytically more succinct, the von Mises distribution.[1,21] For a decently long run the sum in Eq. (1) is then self-averaging.[3] Figure 4 shows that, for instance, von Mises is just the right approach. It is an absolutely continuous distribution that we can use for δ'_j in Eq. (6) and that gives rise to the multiplicative $F(\omega)$ in Eq. (5).

As the input frequency $\nu_\circ$ increases neuronal refractory behavior sets in and spikes are skipped. That is, the ζ_j in Eq. (6) becomes effective. One can even condition the δ'_j with respect to the event $\zeta_j = 1$ occurring the first time, etc. Since skipping can become quite important[9,23] we show in Fig. 5 the 15 single-run plots of the RVS as a function of ν together with the mean number of spikes for four cases of input frequency, viz., $\nu_\circ = 300$, 700, 1000, and 1500 Hz. In so doing, however, we could skip the 300 Hz case ourselves since the two curves exactly agree while not only the arithmetical mean $\langle n\rangle$ but also the actual number of spikes equals 300, as expected for perfect locking since $\nu_\circ = 300$ for $T_{\mathrm{ex}} = 1$ s; cf. Fig. 2.

Analyzing Fig. 5 as $\nu_\circ$ increases gives us a lot of insight into how phase locking behaves and how the number of actually active neurons decreases. Defining the firing fraction $\gamma = \langle n\rangle/N$ we see that γ decreases from 1.0 for $\nu_\circ = 300$ Hz through $\gamma = 0.07$ for $\nu_\circ = 1000$ Hz to $\gamma = 0.02$ for $\nu_\circ = 1500$ Hz. Whereas the RVS of single runs are all identical and handbook-like for $\nu_\circ = 300$, they are not and differ greatly for $\nu_\circ = 1500$ Hz, signaling that phase locking has already become a "hard" job, even though $\mathrm{RVS}(\nu_\circ = 1500) = 0.40$ still seems to indicate a decent locking into $\nu_\circ = 1500$ Hz.

IV. NOISE IN BROWN GHOST ELECTRORECEPTION

In the case of the electroreceptors, we will see that the RVS shows the main features that we expect and noticed in the case of the auditory data. In fact, the raw data of the brown ghost exhibit fundamentally a skipping pattern, as in auditory TB data for high frequencies seen above, particularly Figs. 3 and 5, or auditory afferents.[10] There is a central peak with multiple side lobes. The RVS in Fig. 6 is shown for each of five sections of the raw data. The RVS computed from the whole data at once is shown in black. For each curve, one sees a central peak in all cases, with multiple side lobes located approximately symmetrically about this central peak. The positions of the maxima correspond, as expected from our theory and in analogy to the auditory data analyzed above, to multiples of the inverse of the duration of each section. This is the case also for the brown ghost minima. However, these minima do not go to zero, which is again consistent with the fact that there is strong skipping at this

EOD frequency. Moreover, it is clear that the central peak for each data section occurs at a slightly different location. This suggests that the data are not stationary, in the sense that the EOD frequency fluctuates slightly over time. Such fluctuations can occur behaviorally, but also due to external factors such as the water temperature.

Interestingly, the curve for the whole data set does not show a regular pattern of maxima and minima. The likely reason is that the frequency of the EOD is drifting during the experiment as we just noted in Fig. 6. This can be seen by comparing the positions of the lobes for each section of data: they do not align. A simple independent, identically distributed (iid) noise jitter would again produce a prefactor in the RVS that would not change the positions of the minima. The fact that several of the anticipated minima do not occur where they should, in that they are too much >0, also suggests that there may be special long-range correlations in successive noise jitter values or that they are not always drawn from the same distribution, so that our simple model breaks down. Strong negative correlations between successive interspike intervals are known to exist in this type of data[23] and may play a role. Yet it is known that there are little linear or nonlinear correlations between successive phase jitters.[23]

Furthermore, the basic statistics of p-unit data, such as interspike interval histogram and negative serial correlations can be well reproduced by models with Gaussian white noise added to integrate-and-fire dynamics with a dynamical threshold or adaptation current.[9] Frequency drifts or finer noise correlations may need to be incorporated in models to account for certain data such as those shown here. Figure 7 shows another use for the RVS. Two quantities are plotted as a function of spike index: on the left is the frequency at which the RVS has its maximum, and on the right the value of this maximum. These quantities are estimated using a running average over short windows of the spike train. From this plot, we see that there are fine fluctuations on a rapid time scale in the frequency that maximizes the VS. In addition, the associated strength of the RVS fluctuates as well. There is no clear correlation between these two kinds of fluctuations, although a more detailed analysis of this question could be pursued in future work.

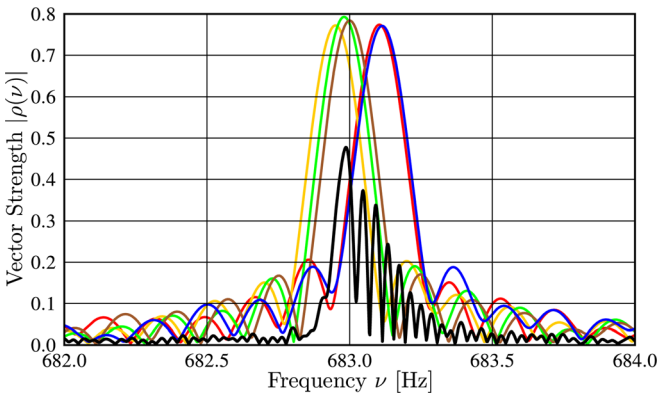

FIG. 6. (Color online) Plot of the RVS $|\rho|$ (vertical axis) as a function of frequency ν (horizontal axis) for a spike train recorded from a p-unit type electroreceptor of the brown ghost (data courtesy of Gary Marsat and Len Maler, Ottawa). The data were recorded for 28.62 s from an afferent nerve at the base of the hindbrain before it enters the skull. The data set consists of 5621 spikes, has been split into 4 equal sections of 1124 and the last of 1125 spikes, and the RVS has been computed as a function of frequency for each section (and plotted while using a different color). The RVS has also been calculated by using the whole data set. See the rather "messy" lower (black) curve with more lobes; it is the absolute value of a convex combination of the above five section sums (1) with weight 1/5. The EOD frequency, which is about 683.0 Hz and drives the receptor, is under the control of the animal and can be determined by such data analysis as the one presented here.

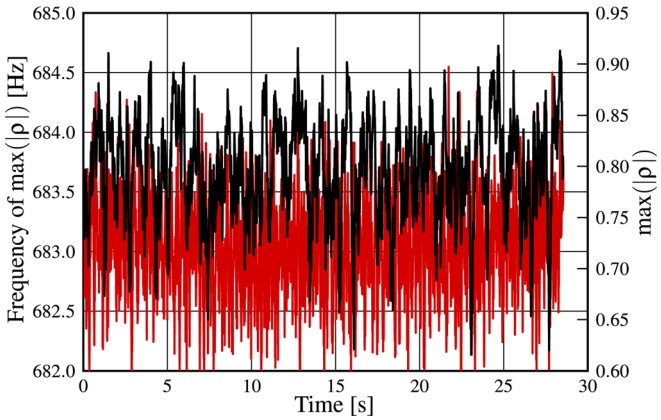

FIG. 7. (Color online) The RVS has been plotted for the electroreceptor data of Fig. 6 using a sliding window of 31 spikes over the spike train. At each spike time, a data set consisting of the preceding 15 and following 15 spikes is used to compute the RVS as a function of frequency. The frequency value at which this RVS is maximal is plotted using the black line (left ordinate axis) and the value of this maximum is plotted using the red line (right ordinate axis). A frequency spacing of 0.002 Hz was used. In passing we note that the RVS maxima in Fig. 6 can be segregated into two different groups of 3 (left) and 2 (right) that effectively correspond to the two different tracks here.

V. DISCUSSION AND OUTLOOK

Chance is a deep notion. Its interpretation started in France of the 18th century and the discussion has been going on ever since. One may well argue[24] that probabilities of events represent our ignorance of the system they belong to because if we knew the system better we could also model it in far more detail or—also possible, as in coin tossing—it is far too difficult to treat it either analytically or numerically. Nevertheless, stochastics allows a highly successful description of reality. Frank Moss was one of those who realized and brilliantly exploited this insight. Stochastic resonance[25] is a most prominent example due in particular to him. It is just our privilege to be truly grateful for his insight.

In the present paper, we have seen how biological systems perform under the influence of a periodic stimulus. To quantify the amount of response periodicity we have used and analyzed the VS, a notion dating back to at least von Mises.[1,3] As the stimulus frequency $\nu_\circ$ increases, the periodicity in the response, if present, in general decreases but the decrease can be taken care of efficiently by a stochastic description. Neuronal skipping and temporally imperfect phase locking have provided a clear illustration, be it in the auditory system of cat or in brown-ghost electroreception.

Of course VS as a quantifier of periodicity is not unique, though it is remarkably simple to formulate; cf. Eq. (1). It is quite appropriate here to mention the "phase synchronization

index" advocated by Moss and coworkers.[20] As usual, the t_k with $1 \le k \le N$ denote spike events. If a neuron fires m times during n cycles of the stimulus, then for $t_k < t < t_{k+1}$ an n:m synchronization is characterized by the phase difference

$$\Phi_{nm}(t) = 2\pi n\left[\frac{t-t_k}{t_{k+1}-t_k}+k\right] - m(2\pi\nu_\circ)t. \tag{8}$$

Denoting the time average over the interval $[0,nT_\circ)$ by $\lfloor \ldots \rfloor$ we put

$$\gamma_{nm}^2 = \lfloor \cos[\Phi_{nm}(\cdot)] \rfloor^2 + \lfloor \sin[\Phi_{nm}(\cdot)] \rfloor^2 \tag{9}$$

One then defines[20] $0 \le \gamma_{nm} \le 1$ to be a "synchronization index" indicative of the relative strength of n:m mode locking with, say, $\gamma_{nm} > 0.1$ as locking criterion. The nonlinear appearance of the spike times t_k as $(t-t_k)/(t_{k+1}-t_k)$ in the exponent already indicates that Eq. (9) is different from Eq. (1) with its $\exp(i\omega_\circ t_k)$ and its being based on another, torus-mapping philosophy.

The RVS technique points to the interesting possibility that a periodically driven neuron exhibits its greatest synchronization—as defined by the classic vector strength—at a frequency slightly different from that of the driving stimulus. This raises the question about the precise combination of deterministic synchronization and stochastic inputs that underlie this effect. It is known from the literature on stochastic phase synchronization[11,20,27] that the noise causes the neuron to become a stochastic oscillator with an internal time scale equal to the mean period of this oscillation. The difference between the firing phase and the driving phase is known to exhibit "plateaus" over certain ranges of input frequency where stochastic phase synchronization is said to occur. Such plateaus reflect the fact that, such as deterministic oscillators, stochastic ones can be entrained to the drive, and thus that the nonlinearities giving rise to phase locking are at play at such higher drive frequencies (at low drive frequencies, the drive is seen more as a modulation, with the result that the firing rate is modulated by the input drive).

Finer details about the mixture of mode-locked patterns contributing to a given firing pattern can be probed with synchronization indices such as Eqs. (8) and (9). In fact, the results in the literature,[11,20,27] particularly Bahar *et al.*,[20] use a varying driving frequency $\nu_\circ$ and compute phase synchronization indices as a function of $\nu_\circ$, as we do here. It may be possible then to modify those measures so that they assess the synchronization to a variable "probing" frequency, as we have done here for the RVS; say, through replacing $\nu_\circ$ in Eq. (8) by ν. It would certainly be of interest to contrast results obtained by their measures[11,20,27] with those from an RVS analysis, which we leave for future work. It may be that the shift between $\nu_\circ$ and the frequency that maximizes RVS is negligible for other systems. Alternately, this shift may be the result of specific mixtures of n:m firing patterns sampled by the noise. Or it may reveal deeper insights into the nature and characteristics of the noise itself, which may in fact partly arise from underlying chaotic behavior.

We can also use entropy[28] for a synchronization criterion. To this end we let $\Pr(0 < t_\ell < T_\circ)$ denote a normalized period-histogram fraction of spike times relative to cyclic stimulation $\omega_\circ$. Furthermore, we weigh the normalized fractions by entropy factors $-\log_2 \Pr(0 < t_\ell < T_\circ)$ so as to obtain the entropy[26] $E = -\sum_\ell \Pr(0 < t_\ell < T_\circ)\log_2 \Pr(0 < t_\ell < T_\circ)$. For a uniform distribution, we find $E_{\max} = \log_2 N$ while plainly $\mathrm{VS} = 0$. We, therefore, define $D = 1 - E/E_{\max}$ to be the period-synchrony criterion with $0 \le D \le 1$. For perfect synchrony the vector strength and D agree $(=1)$ and so they do for a uniform distribution of events $(=0)$. By its very definition D can identify[29] the presence of, e.g., two different periods $T_\circ$ and $T_\circ/2$ and so can RVS in Eq. (1), whereas traditional vector strength cannot as it vanishes identically. Since there is no free parameter such as $\nu_\circ$ in Eq. (8), a direct RVS analog does not exist.

Finally, by mapping discrete spike events t_j that live on the real axis through $t_j \mapsto \exp(i\omega t_j)$ onto the torus and taking their convex combination $n^{-1}\sum_j \exp(i\omega t_j)$ in the unit disk we explicitly show that the vector strength and RVS are geometric methods disjoint from Hilbert transform techniques.

Given the spike events of the neuronal response we have studied the "resonating vector strength" (RVS) $\rho(\nu)$ as a function of the frequency ν as a real variable and shown that in general it exhibits a resonating behavior in the neighborhood of the stimulus frequency $\nu_\circ$. Exploiting its freedom of using frequency as an extra variable for analyzing a given set of events such as spikes, the RVS technique probes deeper and raises new questions about certain fundamental assumptions regarding the role of noise and its coupling to the firing dynamics—and consequently its origin and role in neuronal coding.

In view of, for instance, Fig. 5 we also see that (physics Nobel-prize winner) Phil Anderson was quite right with his famous but apocryphal statement "Thou shalt not average." If quantities are self-averaging, you need not and if they are not, you should not. To see why we can also phrase it in Anderson's own words:[30] "No real atom is an average atom, nor is an experiment ever done on an ensemble of samples." How true.

ACKNOWLEDGMENTS

We cordially thank Philip Joris (University of Leuven) for providing the experimental spike data leading to Figs. 1–5. We further thank Gary Marsat and Len Maler (University of Ottawa) for making available the spike train data from an electroreceptor. We are also greatly indebted to Benedikt Daurer for valuable help in preparing the figures, the Humboldt Foundation for the Humboldt Award to A.L. for his stay at the Technische Universität München, and the Bernstein Center for Computational Neuroscience—Munich for financial support to the third author.

[1] R. von Mises, Phys. Z. **19**, 490 (1918).
[2] J.M. Goldberg and P.B. Brown, J. Neurophysiol. **31**, 639–656 (1969).
[3] J. L. van Hemmen, TUM preprint.
[4] J. L. van Hemmen and A. N. Vollmayr, TUM preprint.
[5] J. L. van Hemmen, in *Handbook of Biophysics*, edited by F. Moss and S. Gielen (Elsevier, Amsterdam, 2001) Vol. 4, pp. 771–823; see in particular Appendices A and B.
[6] P. X. Joris, D. H. Louage, L. Cardoen, and M. van der Heijden, Hearing Res. **216–217**, 19 (2006).

[7]P. X. Joris and P. H. Smith, Neurosci. **154**, 65 (2008).
[8]M. J. Chacron, A. Longtin, and L. Maler, Curr. Opin. Neurobiol. **21**, 752 (2011).
[9]M. J. Chacron, A. Longtin, M. St-Hilaire, and L. Maler, Phys. Rev. Lett. **85**, 1576 (2000).
[10]A. Longtin, A. Bulsara, and F. Moss, Phys. Rev. Lett. **67**, 656 (1991).
[11]A. B. Neiman and D.F. Russell, Phys. Rev. Lett. **88**, 138103 (2002).
[12]A. B. Sichert, R. Bamler, and J. L. van Hemmen, Phys. Rev. Lett. **102**, 058104 (2009)
[13]M. J. Chacron, B. Doiron, L. Maler, A. Longtin, and J. Bastian, Nature (London) **423**, 77 (2003).
[14]M. J. Chacron, L. Maler, and J. Bastian, Nat. Neurosci. **8**, 673 (2005).
[15]J. Lamperti, *Probability* (Benjamin, New York, 1966); 2nd ed. (Wiley, New York, 1996)
[16]H. Dym and H. P. McKean, *Fourier Series and Integrals* (Academic, New York, 1972).
[17]C. Koch, *Biophysics of Computation: Information Processing in Single Neurons* (Oxford University Press, New York, 1999).
[18]M. Konishi, Sci. Am. **268**(4), 34 (1993).
[19]A. Longtin and D. R. Chialvo, Phys. Rev. Lett. **81**, 4012 (1998)
[20]S. Bahar, A. Neiman, L. A. Wilkens, and F. Moss, Phys. Rev. E **65**, 050901(R) (2002).
[21]D. H. Johnson, J. Acoust. Soc. Am. **68**, 1115 (1980).
[22]K. V. Mardia and P. E. Jupp, *Directional Statistics* (Wiley, New York, 1999).
[23]A. Longtin and D. M. Racicot, BioSystems **40**, 111 (1997).
[24]B. de Finetti, *Theory of Probability* (Wiley, London, 1974) Vol. 1.
[25]K. Wiesenfeld and F. Moss, Nature (London) **373**, 33 (1995).
[26]R. B. Ash, *Information Theory* (Wiley, New York, 1965).
[27]M. G. Rosenblum, A. Pikovsky, J. Kurths, C. Schäfer, and P. A. Tass, in *Neuro-Informatics and Neural Modelling*, edited by F. Moss and S. Gielen, Handbook of Biological Physics, Vol. 4 (Elsevier, Amsterdam, 2001), pp. 279–321.
[28]P. A. Tass, M. G. Rosenblum, J. Weule, J. Kurths, A. Pikovsky, J. Volkmann, A. Schnitzler, and H.-J. Freund, Phys. Rev. Lett. **81**, 3291 (1998); the entropy criterion is contained in $\tilde{\rho}_{nm}$.
[29]Y. Kajikawa and T. A. Hackett, J. Neurosci. Methods **149**, 90 (2005).
[30]P. W. Anderson, Nobel Lecture 1977, in *Nobel Lectures Physics, 1971–1980*, edited by S. Lundqvist (World Scientific, Singapore, 1992), pp. 371–398, in particular p. 394.